Time-Periodic Quantum Point Interactions

Taksu Cheon
Kochi University of Technology
Kochi, Japan
e-mail: taksu.cheon@kochi-tech.ac.jp

Sergey Poghosyan
Kochi University of Technology
Kochi, Japan
e-mail: sergey.poghosyan@kochi-tech.ac.jp

ABSTRACT

We show that the quantum particle motion under Dirac's delta function potential with time periodic strength, can be mapped to the motion on a star graph with infinite number of edges and non-convectional node couplings. With suitable finite truncation of number of edges, the problem can be solved analytically, and yields solutions showing intriguing patterns of threshold resonances.

Keywords

Solvable quantum mechanics, time-dependent Schr¨odinger equation, quantum graphs

1. INTRODUCTION

Contact interactions in quantum mechanics offer possibilities to elucidate various intricate phenomena by solvable models [1, 2, 3]. The assemblage of properly tuned closely-placed two and three Dirac's delta interactions on a line is known to produce a so-called delta-prime interaction, an exotic "dual partner" of delta interaction [4]. Periodically placed delta or delta-prime interactions on lattices are simple and solvable models of electron transport in solids [5, 6]. There are some cases when it is useful to consider the strength of the delta function to be a time dependent quantity, instead of a constant [8, 7, 9]. In this article we consider a time-periodic delta interaction, and show that it can be viewed as a realization of quantum graph with non-conventional node couplings. The system possesses a rich structure arising from the threshold resonances with harmonic frequencies of the time-periodicity.

2. PSEUDOENERGY FOR TIME-PERIODIC QUANTUM SYSTEM

Consider a time-dependent Hamiltonian on a one-dimensional space

$$H(t) = -\frac{\hbar^2}{2m}\frac{\partial^2}{\partial x^2} + V(r)f(t) \tag{1}$$

with time periodicity

$$f(t+T) = f(t). \tag{2}$$

The Schrödinger equations

$$i\frac{\partial}{\partial t}\psi(t) = H(t)\psi(t), \tag{3}$$

$$i\frac{\partial}{\partial t}\psi(t+T) = H(t+T)\psi(t+T) \tag{4}$$

along with the time periodicity of the Hamiltonian $H(t+T) = H(t)$ guarantee the existence of pseudo-energy λ which relates $\psi(t+T)$ and $\psi(t)$ by

$$\psi(t+T) = e^{i\lambda T}\psi(t). \tag{5}$$

An alternative expression of (5) is

$$\psi(t) = e^{i\lambda t}\phi(t) \tag{6}$$

in which $\phi(t)$ is T-periodic, namely

$$\phi(t+T) = \phi(t). \tag{7}$$

With the boundary condition (7), the pseudo-energy λ is determined by the eigenequation

$$\left(H(t) - i\frac{\partial}{\partial t}\right)\phi(t) = \lambda\phi(t). \tag{8}$$

Note that we have suppressed the dependence on the spatial coordinate x in the above notations of ψ and ϕ.

3. TIME-PERIODIC DELTA POTENTIAL AND EQUIVALENT QUANTUM GRAPH

To solve the eigenequation (8) for time periodic system, we decompose the wave function ϕ in terms of Fourier time series

$$\phi(x,t) = \sum_n \phi_n(x)e^{in\omega t} \tag{9}$$

with

$$\omega = \frac{2\pi}{T}. \tag{10}$$

The sum in (9) runs over entire integer range from negative to positive infinities, but in actual calculation we need to truncate it by fixed N such that n is confined in between $-N$ and N. We define temporal matrix elements of time-periodic operator $A(t)$ as

$$(m|A|n) = \frac{1}{T}\int_0^\infty dt e^{-im\omega t}A(t)e^{in\omega t}. \tag{11}$$

Some useful examples are

$$(m|n) = \delta_{m,n}, \tag{12}$$

$$(m|\cos\omega t|n) = \frac{1}{2}\left(\delta_{m,n+1} + \delta_{m,n-1}\right), \tag{13}$$

$$(m|\sin\omega t|n) = \frac{1}{2i}\left(\delta_{m,n+1} - \delta_{m,n-1}\right). \tag{14}$$

$$(m|\sum_n \delta(t-nT)|n) = 1. \tag{15}$$

The eigenequation for ϕ takes the form

$$\left(-\frac{\hbar^2}{2m}\frac{\partial^2}{\partial x^2}+n\omega\right)\phi_n(x)+V(x)\sum_n (n|f|m)\,\phi_m(x) = \lambda\phi_n(x). \tag{16}$$

Let us now assume that the potential $V(x)$ is non-zero only in the vicinity of the origin $x=0$. If the relevant wave length is far larger than the active range of $V(x)$, it makes good sense to approximate $V(x)$ by a Dirac's δ-function with appropriate strength

$$V(x)=v\delta(x). \tag{17}$$

With this potential, we can integrate the eigenequation (16) in the infinitely thin range $x=[0_-,0_+]$ and obtain the set of connection conditions at $x=0$ in the form

$$\phi'_n(0_+)-\phi'_n(0_-)=u\sum_{m=-N}^{N} f_{n,m}\phi_m(0_+), \tag{18}$$

$$\phi_n(0_+)-\phi_n(0_-)=0, \tag{19}$$

where we adopted the simplified notation $f_{n,m}=(n|f|m)$ and $u=\frac{2m}{\hbar^2}v$. Everywhere other than $x=0$, the wave function components $\phi_n(x)$ satisfy a decoupled Schrödinger equation

$$\left(-\frac{\hbar^2}{2m}\frac{\partial^2}{\partial x^2}+U_n\right)\phi_n(x)=\lambda\phi_n(x) \tag{20}$$

with constant potentials $U_n=n\omega$. This is nothing but the $(4N+2)$-channel quantum star graph with constant potentials at edges, considered by Turek and Cheon [10, 11]. The channel is specified by integer n and sign σ, for which $\sigma=\pm$ correspond to positive and negative x respectively (Fig. 1).

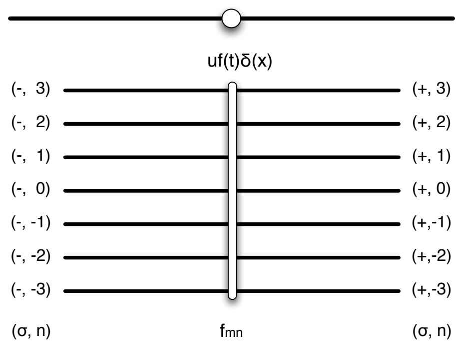

Figure 1: δ interaction with time periodic strength (top) and equivalent quantum graph (bottom)

Table 1. Ordering scheme of channels

(j)	0_σ	n
(1)	$0+$	N
$\vdots$	$\vdots$	$\vdots$
$(2N+1)$	0_+	$-N$
$(2N+2)$	0_-	N
$\vdots$	$\vdots$	$\vdots$
$(4N+2)$	0_-	$-N$

In order to place the connection conditions (18)-(19) in more general setting, we order the Fourier components of $\phi(0_\pm)$ and $\phi'(0_\pm)$ using the new index (j), in the manner given in the table, and define the boundary vectors

$$\Phi=\begin{pmatrix}\phi_{(1)}\\ \vdots\\ \phi_{(4N+2)}\end{pmatrix},\qquad \Phi'=\begin{pmatrix}\phi'_{(1)}\\ \vdots\\ \phi'_{(4N+2)}\end{pmatrix}. \tag{21}$$

The connection conditions (18)-(19) can be expressed in the form

$$A\Phi+B\Phi'=0 \tag{22}$$

with the boundary matrices A and B given in a Turek's TS-form [12]

$$A=-\begin{pmatrix}U^{(2N+1)} & 0^{(2N+1)}\\ -I^{(2N+1)} & I^{(2N+1)}\end{pmatrix},\quad B=\begin{pmatrix}I^{(2N+1)} & I^{(2N+1)}\\ 0^{(2N+1)} & 0^{(2N+1)}\end{pmatrix}, \tag{23}$$

where the matrices $I^{(n)}$ and $0^{(n)}$ have dimension n and are defined as follows

$$0^{(n)}=\begin{pmatrix}0 & \cdots & 0\\ \vdots & & \vdots\\ 0 & \cdots & 0\end{pmatrix},\qquad I^{(n)}=\begin{pmatrix}1 & & 0\\ & \ddots & \\ 0 & & 1\end{pmatrix}. \tag{24}$$

The matrix U holds the information on the interaction matrix elements;

$$U^{(n)}=\begin{pmatrix}uf_{(1),(1)} & \cdots & uf_{(1),(n)}\\ \vdots & & \vdots\\ uf_{(n),(1)} & \cdots & uf_{(n),(n)}\end{pmatrix}. \tag{25}$$

4. THE SCATTERING MATRICES

After fixing the boundary conditions (22) at the graph vertex, we can consider a scattering problem in which there is an incoming wave from the channel specified by $(-,n)$.

$$\psi_n^-(x,t)=\tfrac{1}{\sqrt{k_n}}e^{ik_nx-i(\lambda-n\omega)t} +\textstyle\sum_m \tfrac{1}{\sqrt{k_m}}S^{--}_{m,n}\ e^{-ik_mx-i(\lambda-m\omega)t}(x<0) \tag{26}$$

$$\psi_n^-(x,t)=\sum_m\frac{1}{\sqrt{k_m}}S^{+-}_{m,n}\ e^{ik_mx-i(\lambda-m\omega)t}(x>0) \tag{27}$$

with

$$k_n=\frac{\sqrt{2m(\lambda-n\omega)}}{\hbar}. \tag{28}$$

We can also consider the case of incoming wave from $x=\infty$

$$\psi_n^+(x,t)=\tfrac{1}{\sqrt{k_n}}e^{-ik_nx-i(\lambda-n\omega)t} +\textstyle\sum_m \tfrac{1}{\sqrt{k_m}}S^{++}_{m,n}\ e^{ik_mx-i(\lambda-m\omega)t}\quad(x>0), \tag{29}$$

$$\psi_n^+(x,t)=\sum_m\frac{1}{\sqrt{k_m}}S^{-+}_{m,n}\ e^{-ik_mx-i(\lambda-m\omega)t}(x<0). \tag{30}$$

The factor $\frac{1}{\sqrt{k_m}}$ in front of the m-th channel is there to guarantee the unitarity of the scattering matrix;

$$\sum_{n',\sigma'}\left|S^{\sigma',\sigma}_{n',n}\right|^2=\sum_{n,\sigma}\left|S^{\sigma',\sigma}_{n',n}\right|^2=1. \tag{31}$$

In terms of $\{\phi_m\}$, this is expressed by

$$(\phi_n^-)_m(x)=\frac{1}{\sqrt{k_m}}e^{ik_mx}\delta_{m,n}+\frac{1}{\sqrt{k_m}}S^{--}_{m,n}\ e^{ik_nx}\quad (x<0), \tag{32}$$

$$(\phi_n^-)_m(x) = \frac{1}{\sqrt{k_m}} S^{+-}_{m,n}\; e^{ik_n x} \qquad (x>0), \tag{33}$$

and

$$(\phi_n^+)_m(x) = \frac{1}{\sqrt{k_m}} e^{-ik_m x}\delta_{m,n} + \frac{1}{\sqrt{k_m}} S^{++}_{m,n}\; e^{ik_n x} \qquad (x>0), \tag{34}$$

$$(\phi_n^+)_m(x) = \frac{1}{\sqrt{k_m}} S^{-+}_{m,n}\; e^{-ik_n x} \qquad (x<0). \tag{35}$$

The scattering matrix $\mathcal{S}$ whose $d = (4N+2)$ elements are given by

$$\mathcal{S} = \begin{pmatrix} S^{++}_{N,N} & \cdots & S^{++}_{N,-N} & S^{+-}_{N,N} & \cdots & S^{+-}_{N,-N} \\ \vdots & & \vdots & \vdots & & \vdots \\ S^{++}_{-N,N} & \cdots & S^{++}_{-N,-N} & S^{+-}_{-N,N} & \cdots & S^{+-}_{-N,-N} \\ S^{-+}_{N,N} & \cdots & S^{-+}_{N,-N} & S^{--}_{N,N} & \cdots & S^{--}_{N,-N} \\ \vdots & & \vdots & \vdots & & \vdots \\ S^{-+}_{-N,N} & \cdots & S^{-+}_{-N,-N} & S^{--}_{-N,N} & \cdots & S^{--}_{-N,-N} \end{pmatrix} \tag{36}$$

can be expressed, in terms of ordering indices (j) as

$$\mathcal{S} = \begin{pmatrix} S_{(1),(1)} & \cdots & S_{(1),(4N+2)} \\ \vdots & & \vdots \\ S_{(4N+2),(1)} & \cdots & S_{(4N+2),(4N+2)} \end{pmatrix}. \tag{37}$$

The matrix $\mathcal{S}$ is shown to be given by [11]

$$\mathcal{S} = -(AD^{-1} + iBD)^{-1}(AD^{-1} - iBD) \tag{38}$$

with a diagonal matrix

$$D = \begin{pmatrix} \sqrt{k_{(1)}} & & 0 \\ & \ddots & \\ 0 & & \sqrt{k_{(4N+2)}} \end{pmatrix}. \tag{39}$$

The most practical choice for the incoming channel is $n = 0$. Let us choose the negative side $\sigma = -1$ as an incomig channel. The quantity we are mostly interested in is the transmission and reflection coefficients which are defined by

$$T = \sum_\ell \left|S^{+-}_{\ell,0}\right|^2 = \sum_\ell \left|S^{-+}_{\ell,0}\right|^2. \tag{40}$$

$$R = \sum_\ell \left|S^{--}_{\ell,0}\right|^2 = \sum_\ell \left|S^{++}_{\ell,0}\right|^2. \tag{41}$$

We can isolate the "elastic" component as

$$T = \left|S^{+-}_{0,0}\right|^2 + \Delta_T, \qquad R = \left|S^{--}_{0,0}\right|^2 + \Delta_R, \tag{42}$$

with the definition

$$\Delta_T = \sum_{\ell\neq 0} \left|S^{+-}_{\ell,0}\right|^2, \qquad \Delta_R = \sum_{\ell\neq 0} \left|S^{--}_{\ell,0}\right|^2. \tag{43}$$

Since we have

$$S^{+-}_{0,0} = 1 + S^{--}_{0,0}, \qquad S^{--}_{\ell,0} = S^{+-}_{\ell,0} \qquad (\ell \neq 0), \tag{44}$$

with the vertex couplings given in the form (23), we obtain

$$\Delta_T = \Delta_R = \frac{1 - |S^{--}_{0,0}|^2 - |S^{+-}_{0,0}|^2}{2}, \tag{45}$$

and we have

$$T = \frac{1 - |S^{--}_{0,0}|^2 + |S^{+-}_{0,0}|^2}{2} = 1 + \Re S^{--}_{0,0}, \tag{46}$$

$$R = \frac{1 + |S^{--}_{0,0}|^2 - |S^{+-}_{0,0}|^2}{2} = -\Re S^{--}_{0,0}. \tag{47}$$

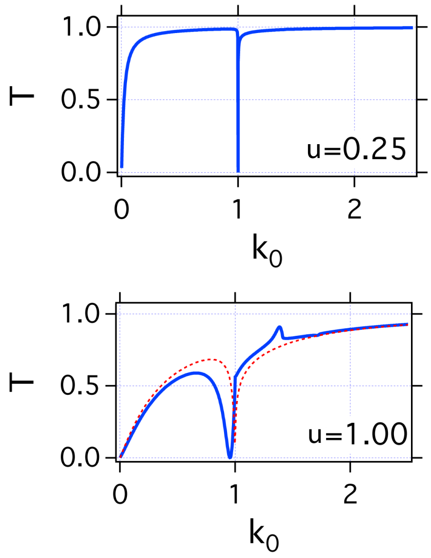

Figure 2: Transmission probability $T(k)$ for $u = 0.25$ (top) and $u = 1.00$ (bottom) with truncations $N = 1$ (dashed line) and $N = 4$ (full line). For the case $u = 0.25$ the truncation effect cannot be seen from the figure.

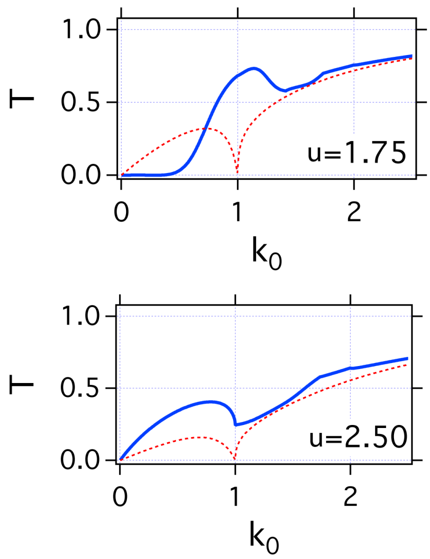

Figure 3: Transmission probability $T(k)$ for $u = 1.75$ (top) and $u = 2.50$ (bottom) with truncations $N = 1$ (dashed line) and $N = 4$ (full line).

5. NUMERICAL EXAMPLES

In this section we assume $f(t) = \cos\omega t$ and show that the transmission amplitude T vacillates as a function of k_0 (Figs. 2 and 3). The effect of truncation at $n = \pm N$ can be discerned from the difference between dashed lines($N = 1, d = 4N+2 = 6$) and full lines ($N = 4, d = 4N+2 = 18$). It can be seen that the truncation at $N = 1$ is already rather good up to around $k\ \sqrt{\omega/\hbar}$ for reasonably small values of u.

These results show that there is a threshold resonance effect at $\lambda = n\omega$. Also, wide variety of k dependence of T and R are observed for different range of k and different values of the coupling constant u. For example, for small $k < \sqrt{\omega}/\hbar$, T can be large for small u and almost zero for large u. There is always a sudden drop of T at the threshold $k = \sqrt{\omega}/\hbar$, and then a sharp increase of transmission. For large u around $u = 4$ scattering features can be used for spectral filtering with the proper choice of ω, for example.

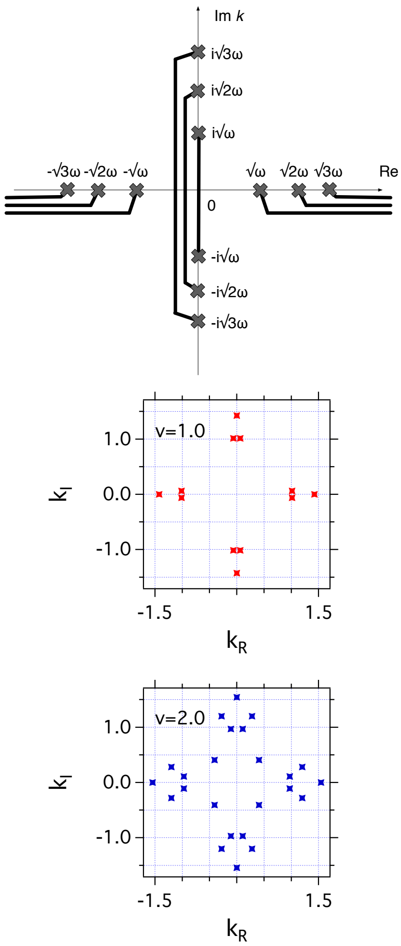

Figure 4: Structure of Riemann surface (top) and positions of poles for $u = 1$ and $u = 2$ (middle and bottom respectively).

The rich structure of the scattering matrix is the result of the complex Riemann surface on which it resides. Compared to the case of time-invariant delta potential, for which the Riemann surface is a single sheet plane and there is a pole on the imaginary axis $k = iu$, the time-periodic variation of the strength u gives a multi-valued scattering matrix whose Riemann surface is illustrated in Fig. 4.

There are various poles both along imaginary and real axes and also off the axes, residing on various sheets of the Riemann surface. Among these poles the "visible" ones are the branch points $k = \sqrt{n\omega}$ located on the real axis, i.e., the physical sheet. Positions of the poles are illustrated in Fig. 4 for different values of u.

ACKNOWLEDGEMENT

We thank Dr. Hirokazu Kobayashi for stimulating discussions during which he has suggested us to explore time-periodic contact interactions in quantum mechanics. This research was supported by the Japan Ministry of Education, Culture, Sports, Science and Technology under the Grant number 24540412.

REFERENCES

[1] S. Albeverio, F. Gesztesy, R. Høegh-Krohn, and H. Holden "Solvable models in quantum mechanics", 2nd ed. with appendix by P. Exner, AMS Chelsea, R. I., 2005.

[2] P. Exner, J.P. Keating, P. Kuchment, T. Sunada, and A. Teplyaev, eds. "Analysis on Graphs and Applications", AMS Proc. of Symposia in Pure Math, Ser., vol. 77, Providence, R.I., 2008.

[3] G. Berkolaiko and P. Kuchment "Introduction to Quantum Graphs, Mathematical Surveys and Monographs", No. 186, AMS Bookstore, 2013.

[4] T. Cheon and T. Shigehara, "Realizing discontinuous wave functions with renormalized short-range potentials", *Phys. Lett. A*, vol. 243, pp. 111-116, 1998.

[5] R. de L. Krönig and W. G. Penney, "Quantum mechanics of electrons in crystal lattices", *Proc. Roy. Soc. (London) A*, vol. 130, pp. 499-513, 1931.

[6] P. Exner, "Lattice Kronig-Penney model", *Phys. Rev. Lett. 74*, pp. 3503-3506, 1995.

[7] M. Mangin-Brinet, J. Carbonell, and C. Gignoux, "Exact boundary conditions at finite distance for the time-dependent Schrödinger equation", *arXiv.org:quant-ph*, 9804030 (8 pp.), 1998.

[8] T. P. Grozdanov and P. S. Krstic, "Distortion of a model atom in intense, high-frequency laser field of linear polarization", *Phys. Lett. A*, vol. 149, pp. 144-150, 1990.

[9] M. A. Andreata and V. V. Dodonov, "Tunnelling of narrow Gaussian packets through delta potentials", *J. Phys. A: Math. Gen.*, vol. 37, pp. 2423-2438, 2014.

[10] O. Turek and T. Cheon, "Threshold resonance and controlled filtering in quantum star graphs", *Europhys. Lett.*, vol. 98, 50005 (5 pp.) 2012.

[11] O. Turek and T. Cheon, "Potential-controlled filtering in quantum star graphs", *Ann. of Phys. (NY)*, vol. 330, pp. 104-141, 2013.

[12] T. Cheon, P. Exner and O. Turek, "Approximation of a general singular vertex coupling in quantum graphs", *Ann. Phys. (NY)*, vol. 325, pp 548578, 2010.